Supporting Information

Reversible polymorph-to-amorphous phase transformation based on an aggregation-dependent thermally activated delayed fluorescence emitter

Jianai Chen,[†] Xingshun Yang,[†] Xinjie Xu,[†] Mingjiao Sun,[†] Rule Zhang,[†] Dongcheng Li,[†] Linjie Ma,[†] Yujie Dong,*[,†] Weijun Li*[,†] and Fener Chen*[,†,‡]

[†] Institute of Pharmaceutical Science and Technology, College of Chemical Engineering, Zhejiang University of Technology, Hangzhou 310014, P. R. China; State Key Laboratory of Green Chemical Synthesis and Conversion, Zhejiang University of Technology, Hangzhou 310014, China.

[‡]Engineering Center of Catalysis and Synthesis for Chiral Molecules, Department of Chemistry, Fudan University, 220 Handan Road, Shanghai, 200433, PR China.

Keywords: multifunction, polymorph-to-amorphous, information encryption, TADF

***Corresponding Author**

E-mail: dongyujie@zjut.edu.cn; liwj@zjut.edu.cn; rfchen@fudan.edu.cn

Supporting Information

Table of Contents

1. Synthesis

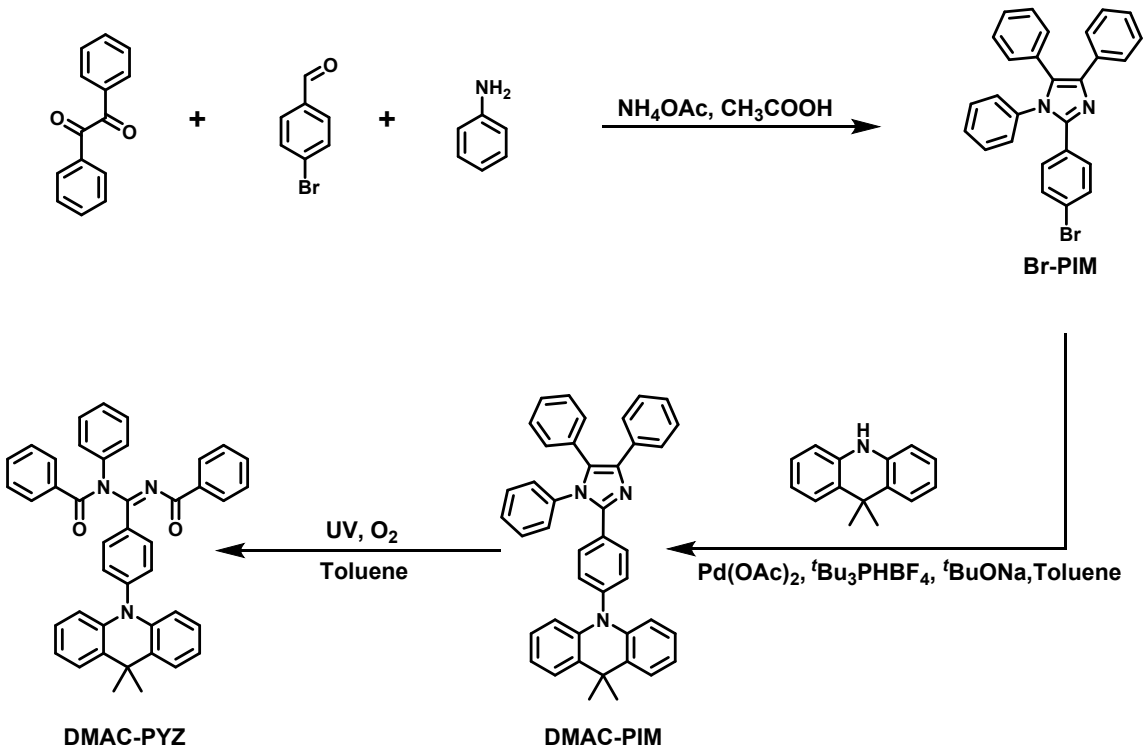

Scheme S1. The synthesis of DMAC-PYZ.

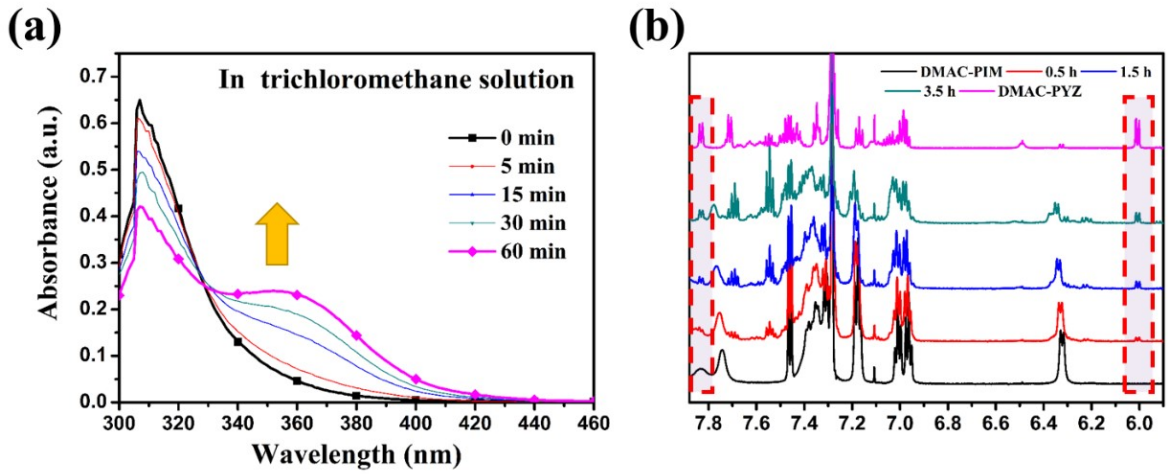

Figure S1. (a) In situ absorption spectra of DMAC-PIM in trichloromethane solvent at 10^{-5} mol L^{-1} under different UV irradiation (365 nm, 6 w) time in air (O_2). (b) The in situ ^1H NMR spectra of DMAC-PIM in $CDCl_3$ solvents under UV irradiation for different time with that of DPA-PYZ used as reference.

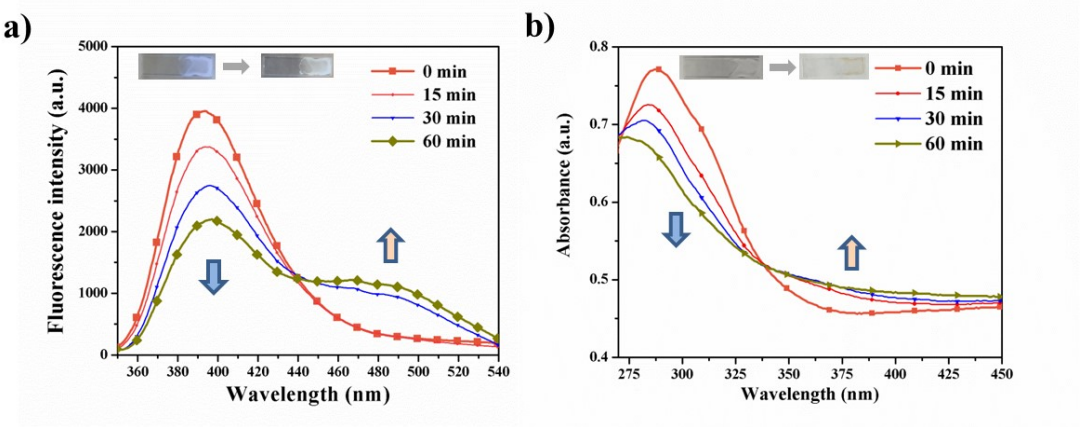

Figure S2. In situ fluorescence spectra (a) and absorption spectra (b) of DMAC-PIM in PMMA film under different UV irradiation (365 nm, 6 w) time in air (O_2).

2. Molecular packing of DG and DY

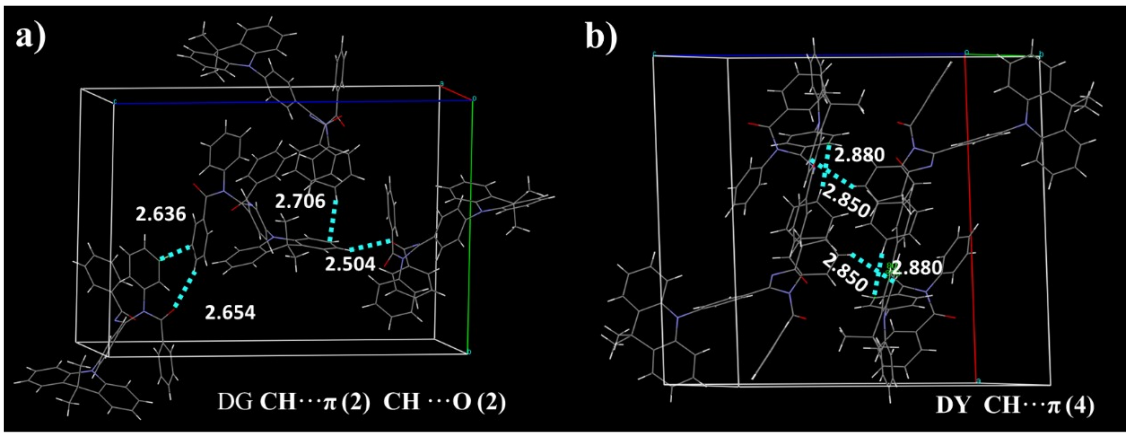

Figure S3. The unit cell of DG and DY single crystals.

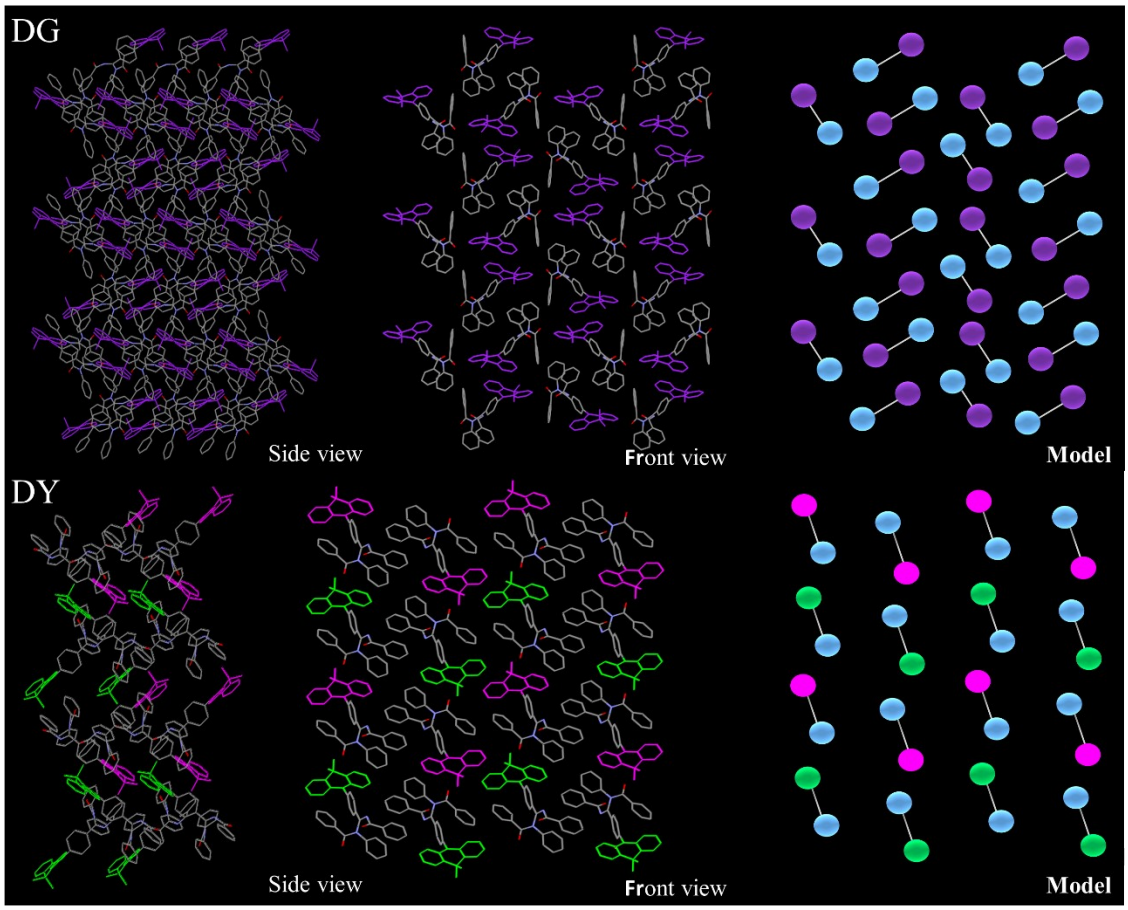

Figure S4. Molecular packing of DG and DY.

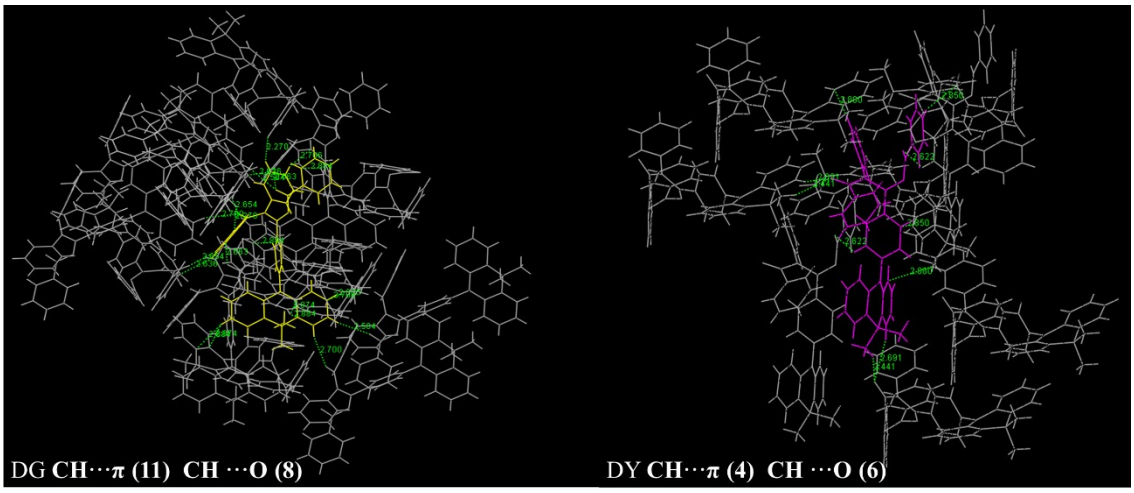

Figure S5. Molecular packing of DG and DY.

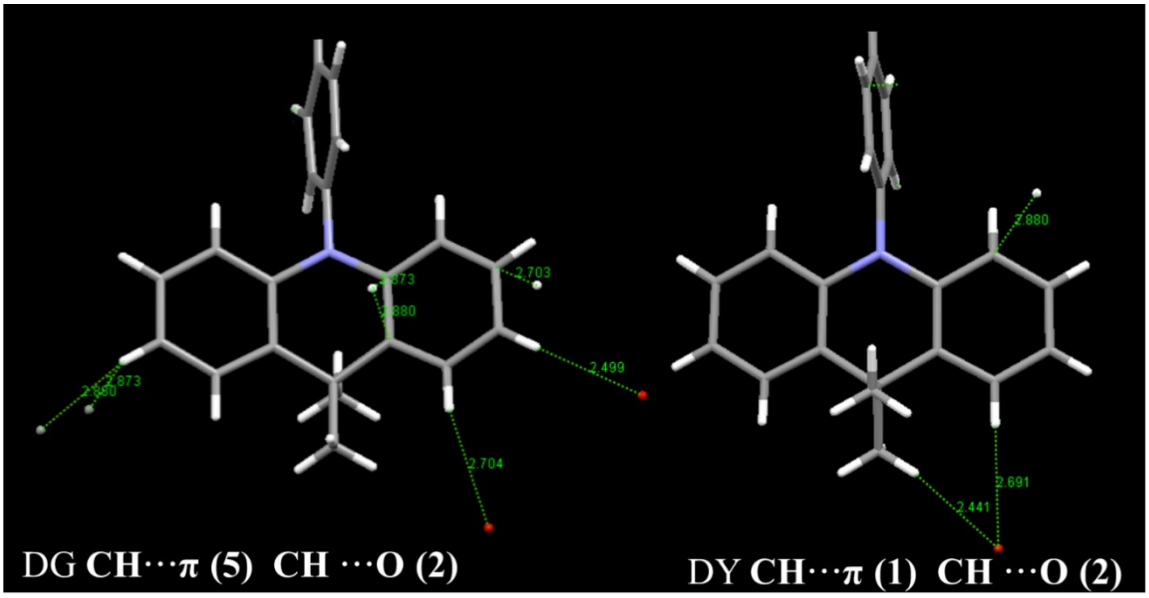

Figure S6. Molecular packing of DMAC moiety of DG and DY DFT of DG and DY.

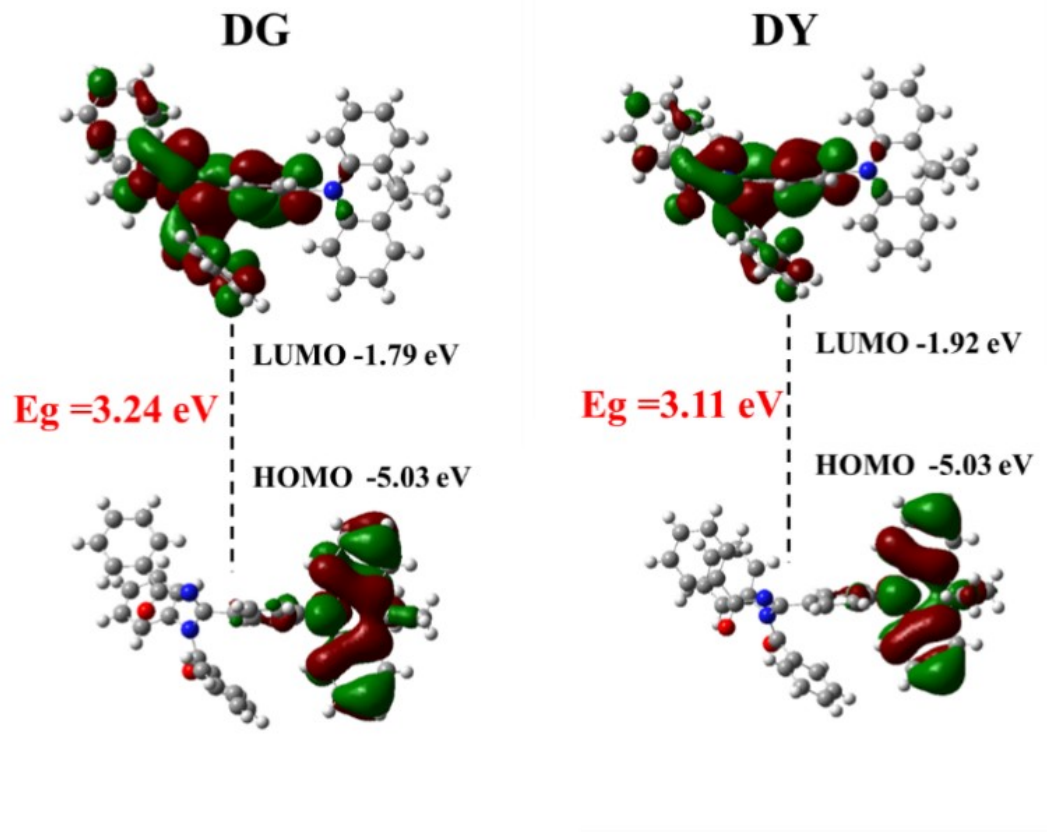

Figure S7. Diagram of theoretical calculated frontier orbital contribution based on B3LYP-6-31g of DG and DY.

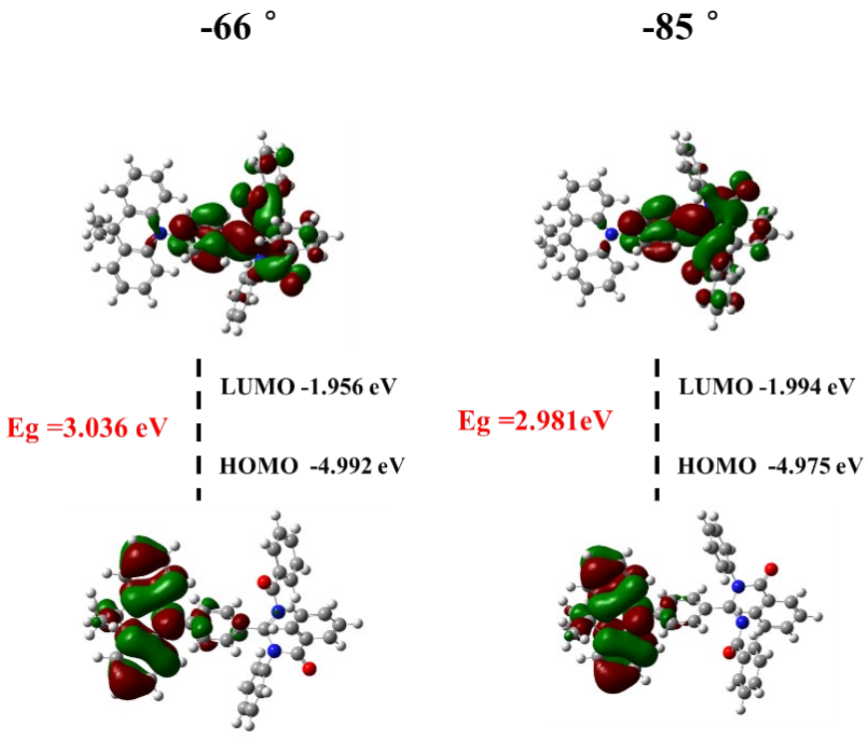

Figure S8. Diagram of theoretical calculated frontier orbital contribution based on B3LYP-6-31g of DMAC-PYZ with the -66° and-85° twisted angle between donor and acceptor group.

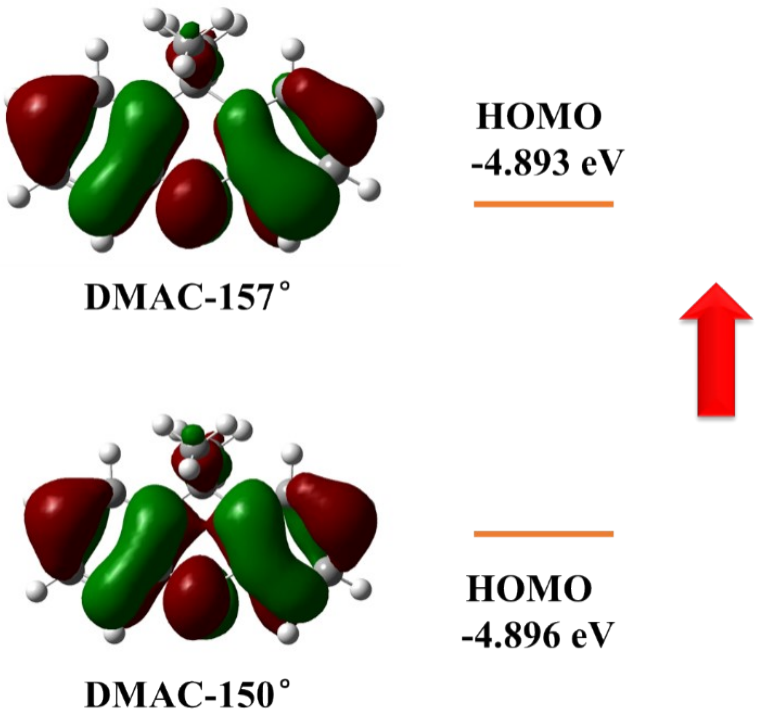

Figure S9. Diagram of theoretical calculated frontier orbital contribution based on B3LYP-6-31g of DMAC donor group with the 157° and 150° dihedral angle.

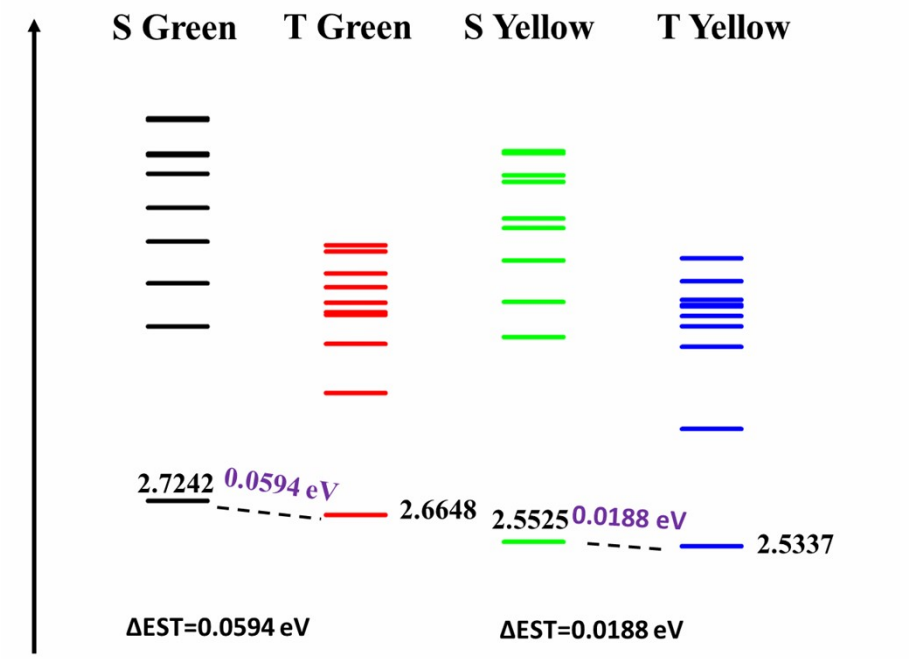

Figure S10. Energy level diagram for singlet and triplet excited states calculated with TD-DFT: m062x/6-31g (d, p).

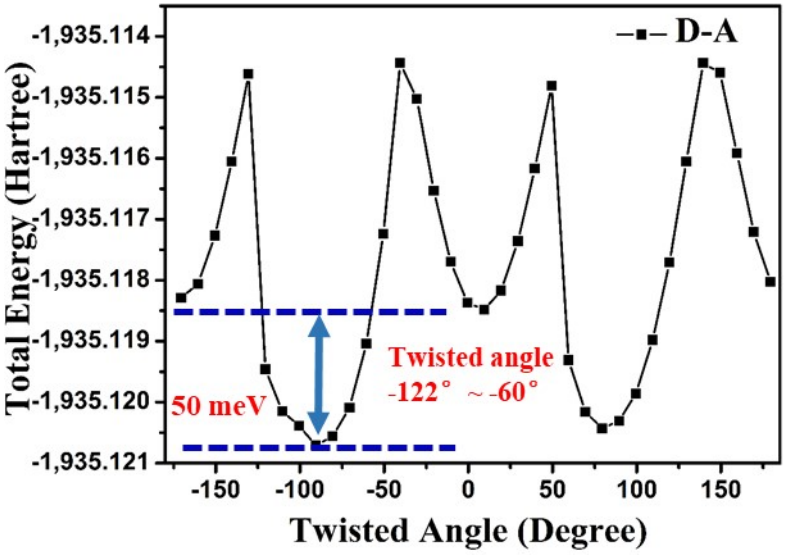

Figure S11. The ground state energy of DMAC-PYZ at different twist angles between DMAC donor and PYZ acceptor in the gas phase using the B3lyp method.

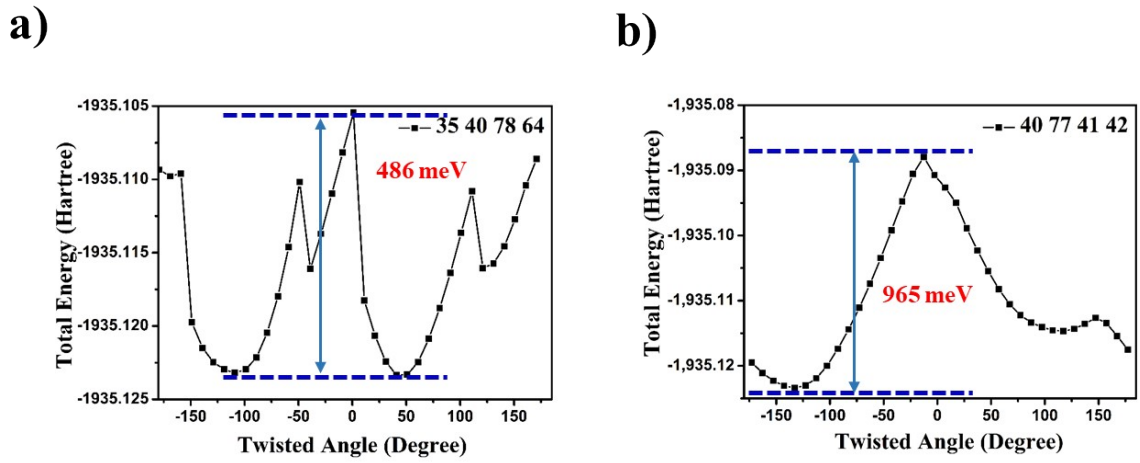

Figure S12. The ground state energy of step 1 a) and Step 2 b) during the conversion between S-Y and R-Y in the gas phase using the B3lyp method.

3. PL spectra and Lifetime measurement of DMAC-PYZ

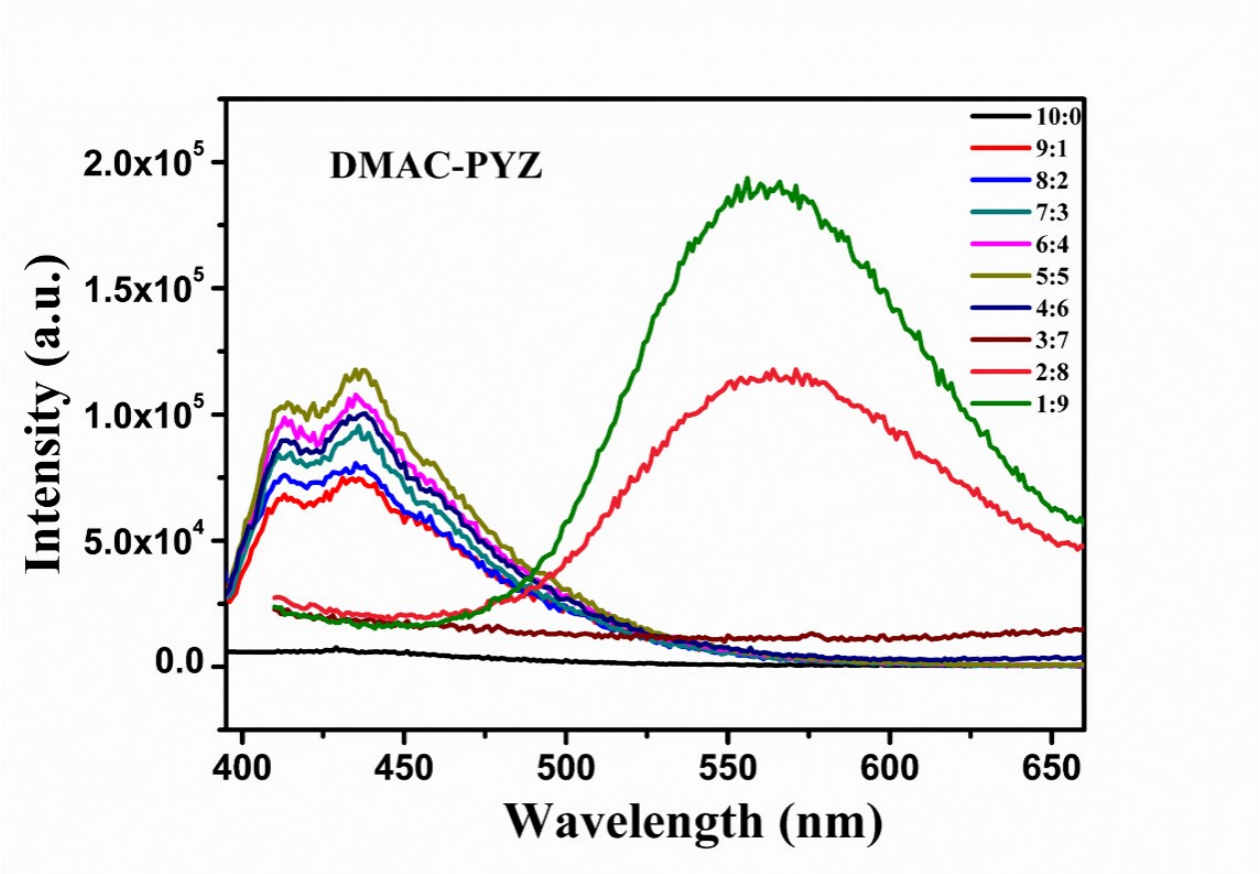

Figure S13. Fluorescence spectra of DMAC-PYZ in the THF: water mixtures (10^{-5} M).

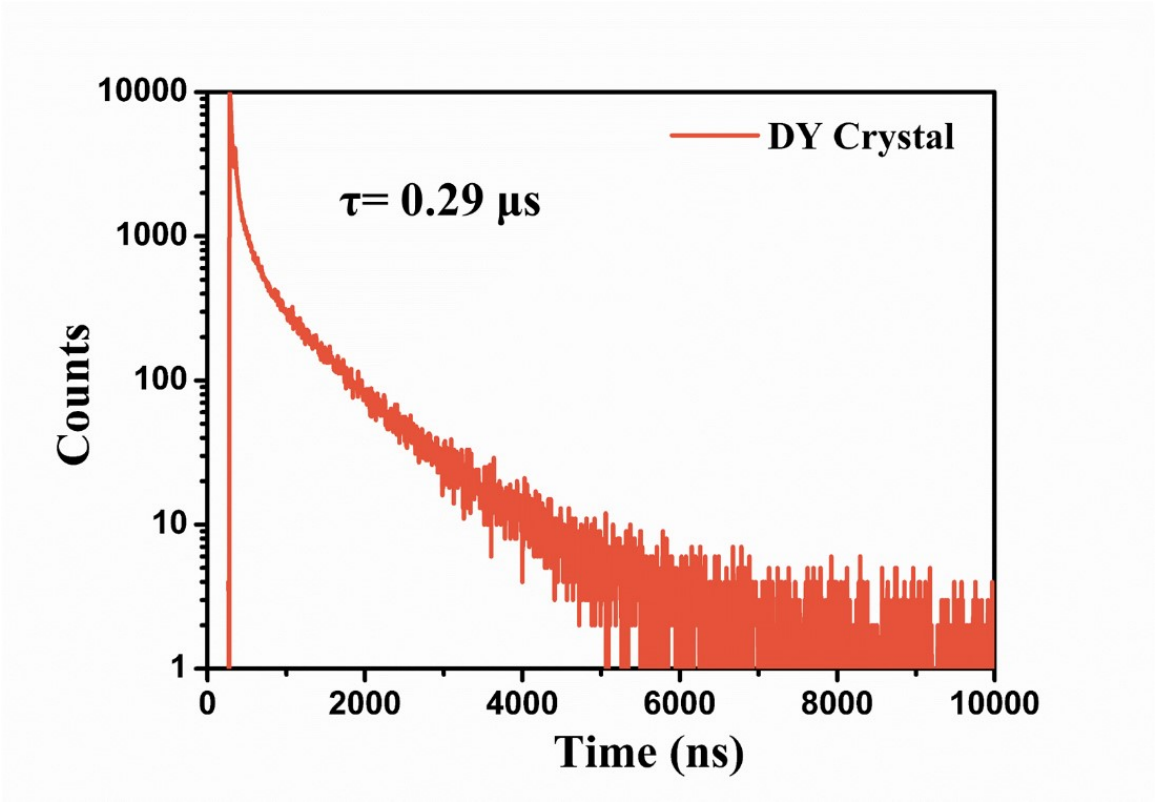

Figure S14. Lifetime measurement of crystals of DY measured at 540 nm.

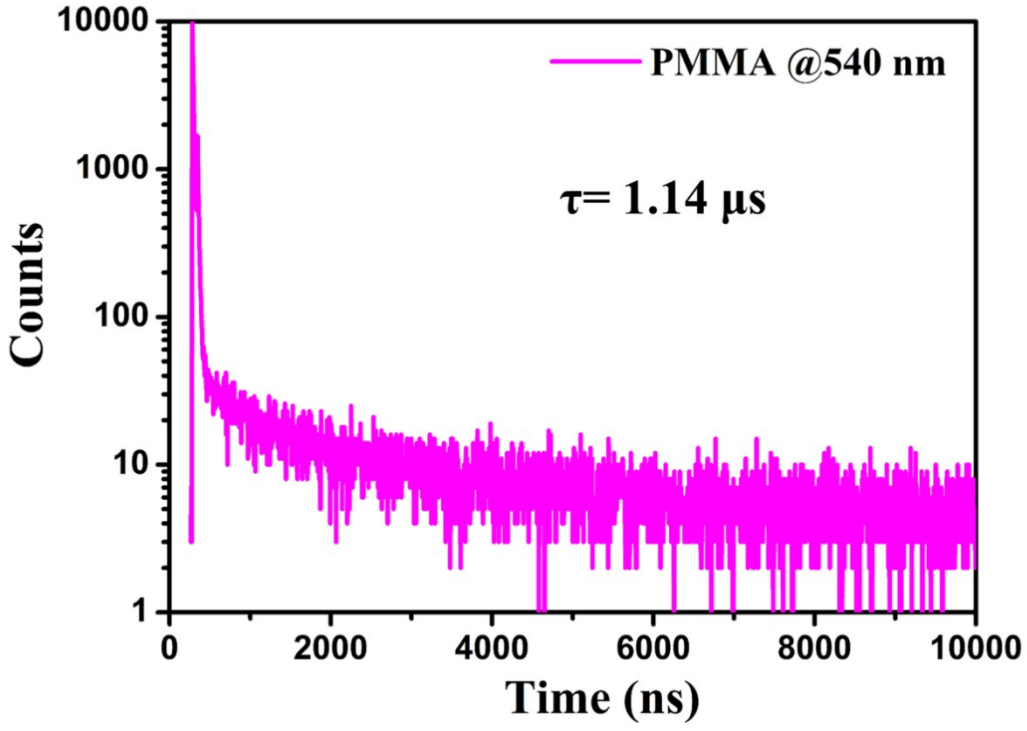

Figure S15. Lifetime measurement of DMAC-PYZ in PMMA doped film.

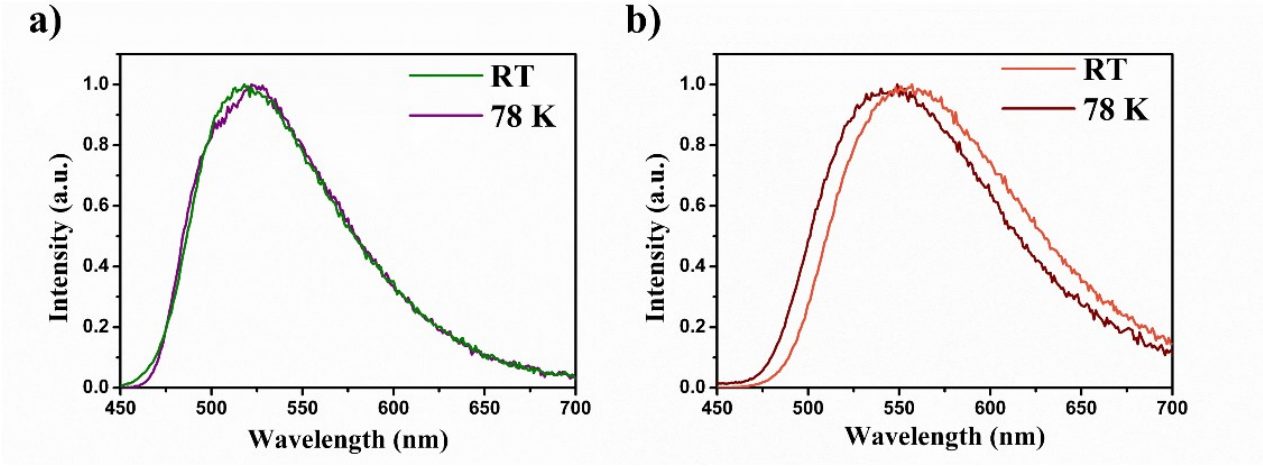

Figure S16. Fluorescence spectra of DG (a) and DY (b) at room temperature and 77 K.

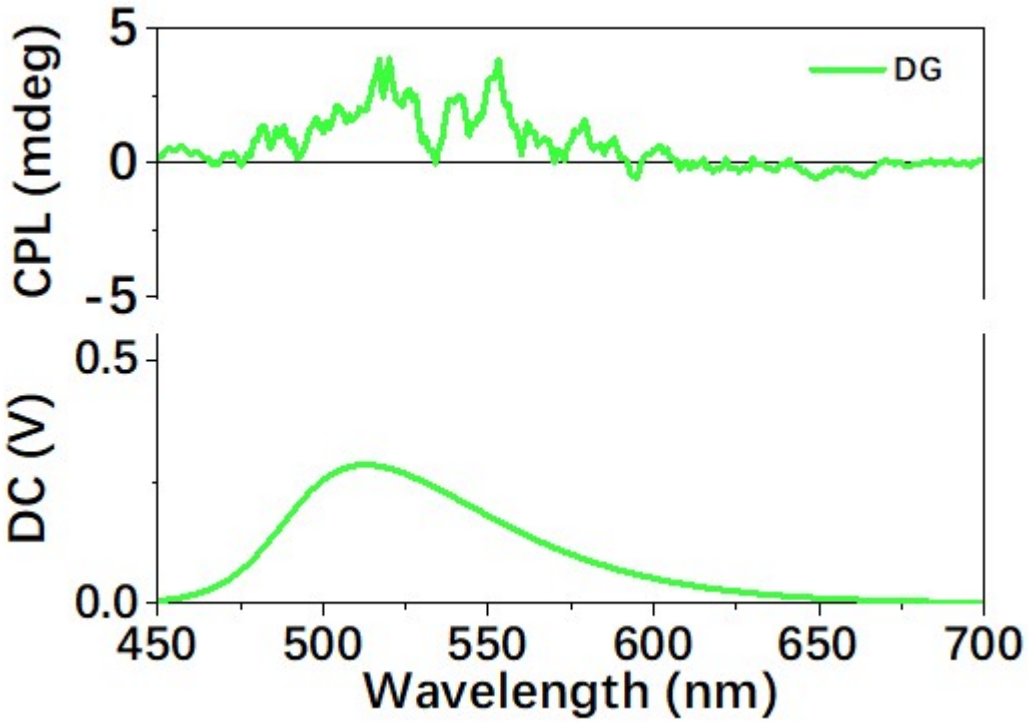

Figure S17. The CPL spectra of crystal DG.

4. Mechanochromism Experiments

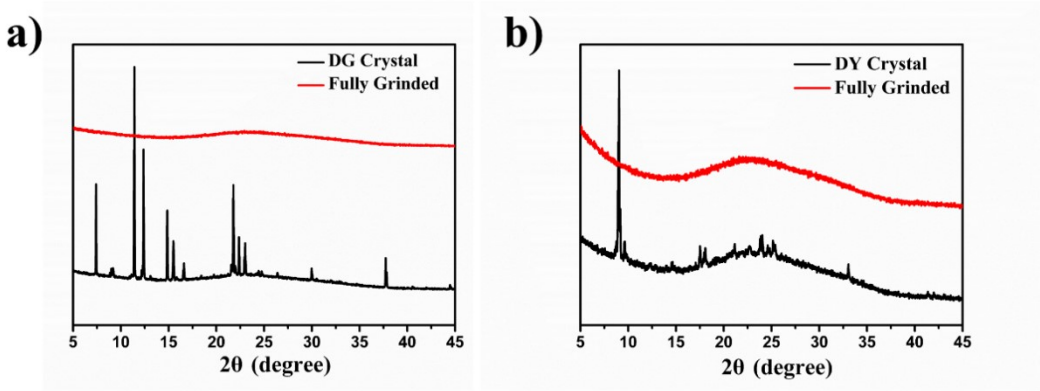

Figure S18. Powder X-ray diffraction (PXRD) data of DG (a) and DY (b) in the different solid states.

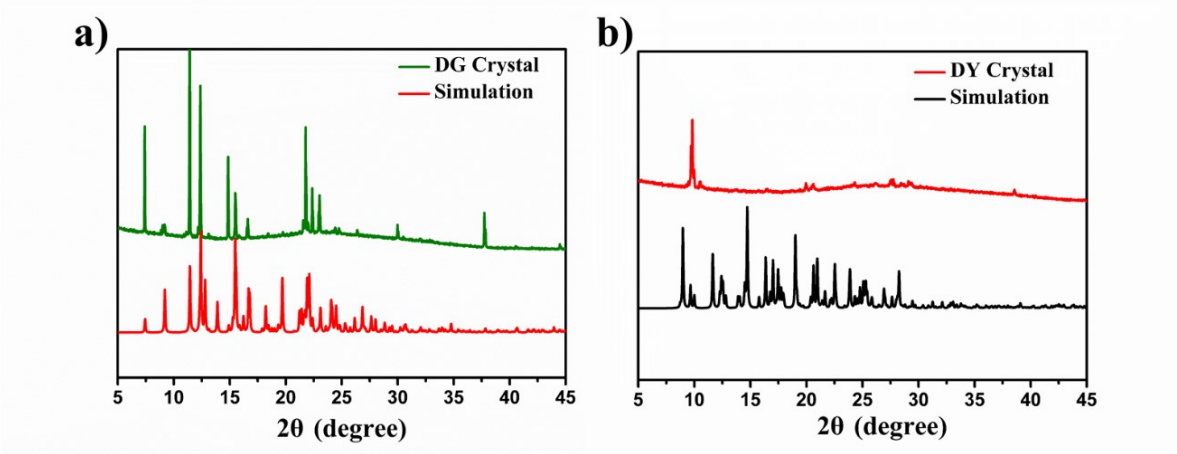

Figure S19. Powder X-ray diffraction (PXRD) data (with that simulated from single crystal structure as reference)

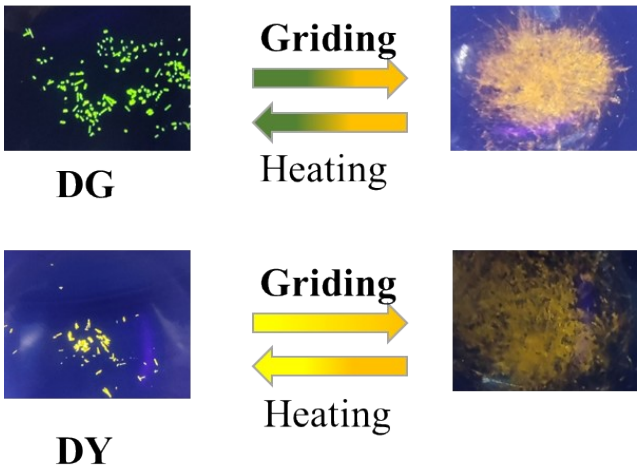

Figure S20. Photos of DG and DY under UV illumination under mechanical force and 60 ℃ thermal stimulation.

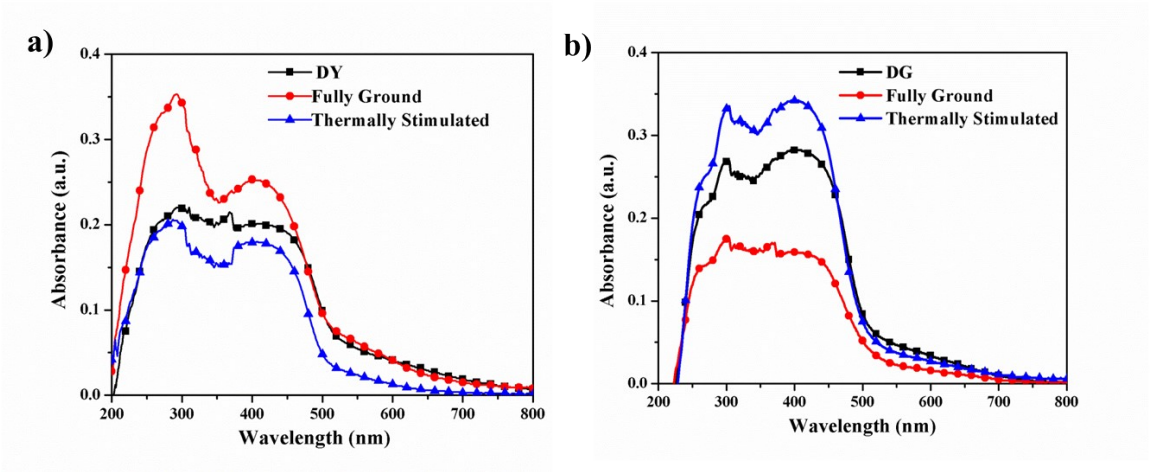

Figure S21.The Solid ultraviolet absorption spectra of amorphous DY a) and DG b) under mechanical force and 60 ℃ thermal stimulus.

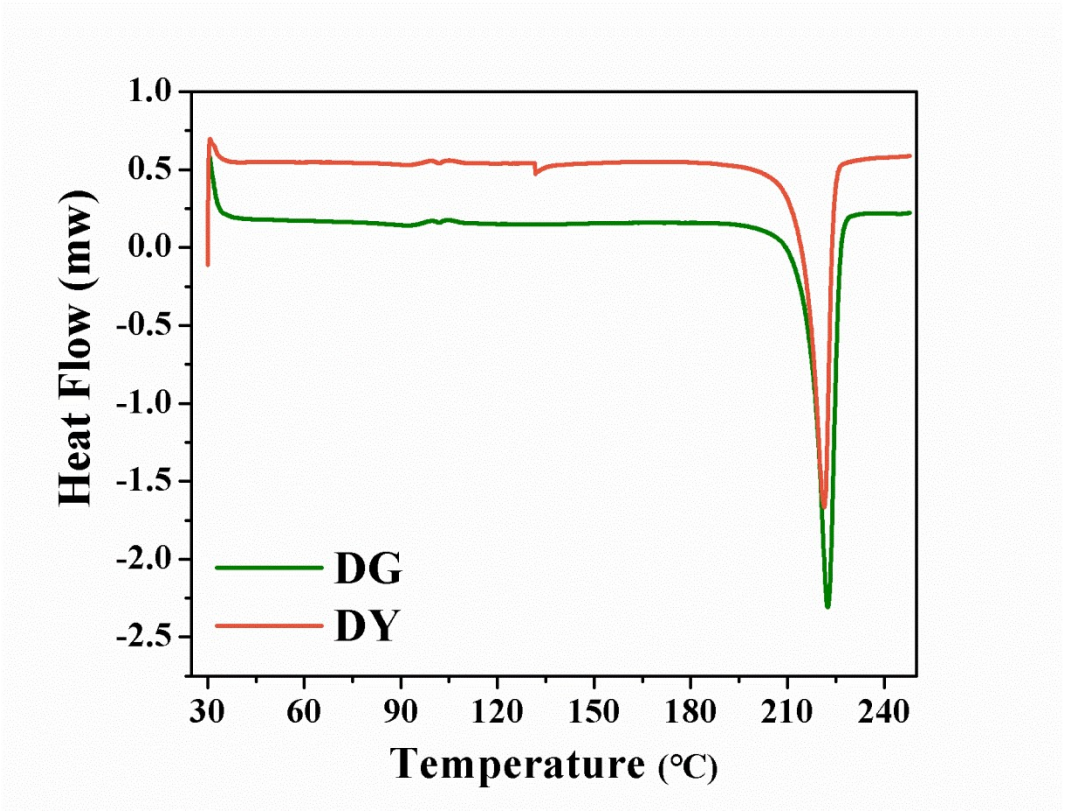

Figure S22. The DSC of the crystalline powders of DG and DY.

Table S1. Photo-physical data of DG and DY.

Compound	λ_{em} [nm][a]	t [μs][a]	Φ_p [%][b]
DG	507	65.76	45.6
DY	540	0.29	6.1

[a] The lifetimes of fluorescence. [b] The fluorescence PLQY under oxygen conditions.

Table S2. Crystal Data and Structure Refinements of Two Crystals

	DG	DY
CCDC No.	2102068	2102069
empirical formula	$C_{42}H_{33}N_3O_2$	$C_{42}H_{33}N_3O_2$
formula wt	611.71	611.71
T, K	296(2)	296(2)
crystal system	orthorhombic	monoclinic
space group	P 21 21 21	P 21/c
a, Å	8.4928(12)	19.704(4)
b, Å	16.372(2)	8.1962(17)
c, Å	23.775(3)	20.230(4)
α,deg	90	90
β,deg	90	92.408(4)
γ,deg	90	90
V,Å3	3305.9(8)	3264.2(12)
Z	4	4
density, Mg/m^3	1.231	1.245
M (Mo K α), mm^{-1}	0.076	0.077
θ range, deg	2.63-18.65	2.827-24.998
no. of reflcns collected	18343	16011
no. of unique reflcns	6492	5726
R(int)	0.0634	0.0539
GOF	0.972	0.918
R1 [I > 2σ(I)]	0.0570	0.0549
wR2 [I > 2σ(I)]	0.1109	0.1300
R1 (all data)	0.1467	0.1133
wR2 (all data)	0.1445	0.1618